Ocean Engineering 152 (2018) 223–233

Contents lists available at ScienceDirect

Ocean Engineering

journal homepage: www.elsevier.com/locate/oceaneng

Cavitation limits on tidal turbine performance

Aidan Wimshurst *, Christopher Vogel, Richard Willden

Department of Engineering Science, University of Oxford, Parks Road, OX1 3PJ, UK

A R T I C L E I N F O

Keywords:
Cavitation
Blockage
Spanwise flow
Safety margin
Tidal turbines

A B S T R A C T

Blockage effects are currently not accounted for in cavitation analyses of tidal turbine rotors. At higher blockage ratios, rotors are more heavily loaded and have potentially stronger suction peaks, so cavitation inception is more likely. In this paper, blade resolved computations are used to carry out a cavitation analysis over a range of blockage ratios and tip-speed-ratios. Our analysis suggests that increasing the blockage ratio from 0.01 to 0.197 reduces the minimum static pressure head in the fluid by approximately 0.5 m. To mitigate this reduction, either the submersion depth of the rotor can be increased or the maximum permissible tip speed ratio reduced. However, reducing the maximum permissible tip speed ratio is shown to severely restrict the rotor thrust and power. Spanwise flow effects are shown to reduce the strength of the suction peak on the outboard blade sections, reducing the likelihood of cavitation inception. Blade element based methods are shown to inadequately account for spanwise flow effects and thus are overly-conservative. Hence, rotors designed with these methods could potentially be operated at higher tip-speed-ratios or reduced submersion depths.

1. Introduction

There is a general desire to increase the design tip-speed-ratio of tidal turbine rotors, which is often around 4–6 and is much lower than the design tip-speed-ratio of utility-scale wind turbines (7–11). Higher design tip-speed-ratios increase the maximum theoretical power coefficient that can be achieved by the rotor and also reduce the maximum torque load, so that a lighter drive train can be adopted with a reduced structural cost (Ning and Dykes, 2014). However, unlike onshore wind turbines (where the tip-speed-ratio is limited by noise constraints), the tip-speed-ratio of tidal turbine rotors is limited by the onset of cavitation.

Bahaj et al. (2007) and Wang et al. (2007) observed the onset of tip vortex cavitation in cavitation tunnels downstream of their experimental tidal turbine rotors. Reducing the static pressure in the tunnel led to the inception of back sheet cavitation on the suction surface of the rotor blade and increased the strength of the tip vortex cavitation. While these experiments are useful for classifying the type of cavitation and observing its onset, tidal turbines need to be designed to avoid the onset of cavitation altogether (DNV GL, 2015). The majority of tidal turbine rotor design algorithms that have been adopted are based on the Blade Element (BE) method, where the rotor blade is divided into several independent aerofoil sections along the span. The forces acting on each aerofoil section are assumed to arise only from the flow components in the plane of the aerofoil section. In the Blade Element Momentum (BEM) method, the BE method is combined with linear and angular momentum conservation equations for each annulus of the rotor disc, to compute the spanwise variation of the angle of attack and relative velocity magnitude (Burton et al., 2011). Batten et al. (2008) used this method to design a tidal turbine rotor, with a cavitation bucket type analysis (originally used in propeller design) to assess the onset of cavitation. This algorithm has subsequently been adopted by other authors to design tidal turbine rotors, including Goundar and Ahmed (2013) and Grogan et al. (2013).

However, algorithms based on the BEM method are only able to design rotors for optimum operation in unblocked conditions (where the device is operating in relative isolation from flow boundaries and other devices). In practice, tidal turbine rotors are likely to be grouped closely together in arrays, allowing them to utilise the increased blockage provided by the free surface, sea bed and other neighbouring devices (Adcock et al., 2015; Vennel et al., 2015). The increased blockage leads to a greater static pressure drop in the streamwise direction across the device (than occurs in unblocked conditions), so the device can support greater thrust and extract more power from the flow. Under these conditions, optimum rotors need to be designed to apply greater thrust to the flow than in unblocked conditions, so that they can extract the increased power that is available (Schluntz and Willden, 2015). McIntosh et al. (2011) proposed an algorithm to design tidal turbine rotors specifically for operation under blocked conditions. Rather than combining the BE method with algebraic momentum equations, they embedded the BE method within a 3D RANS

* Corresponding author.
E-mail address: Aidan.Wimshurst@eng.ox.ac.uk (A. Wimshurst).

https://doi.org/10.1016/j.oceaneng.2018.01.060
Received 12 October 2017; Received in revised form 9 December 2017; Accepted 13 January 2018
Available online 23 February 2018

solver, which can account for blockage directly through the boundary conditions of the domain. When operated at the blockage ratio they were specifically designed for, rotors that were designed for blockage have been shown to universally outperform rotors that were not designed specifically for that blockage condition (Schluntz and Willden, 2015).

Despite the adoption of these BE based design algorithms, the effect of blockage on cavitation inception has not been examined directly. With increasing blockage ratio, rotors are more heavily loaded, can produce higher power and have potentially stronger suction peaks. Hence, rotors are more likely to cavitate at higher blockage ratios, since the minimum static pressure in the fluid is reduced. Furthermore, blade resolved computations performed by Wimshurst and Willden (2017) have observed significant spanwise flow (40–50% of the freestream velocity) on the outboard sections of tidal turbine rotor blades. This spanwise flow changes the surface pressure distribution on the outboard blade sections and reduces the strength of the suction peak. As the magnitude of the suction peak reduces, the minimum static pressure in the fluid increases, so the fluid is less likely to cavitate. Hence, BE based design algorithms that do not adequately account for spanwise flow effects are likely to inaccurately predict cavitation inception.

In this work, a cavitation analysis will be carried out using a series of blade resolved computations, which account for blockage and spanwise flow effects directly. The results of these computations will be compared with the results of a separate cavitation analysis carried out with a BE based method, to quantify the discrepancies in the BE method. In addition, a hydrodynamic safety margin will be proposed and included in the analysis to account for ambient turbulence, free surface waves and velocity shear (which are not modelled explicitly). This safety margin increases the minimum allowable static pressure on the suction surface of the blade, to account for the unsteady pressure fluctuations which have not been modelled. It can be realised in practice by either reducing the maximum permissible tip-speed-ratio of the rotor or increasing the depth of submersion. To complete the analysis, the resulting restriction on the range of thrust and power coefficients that can be achieved by the rotor will be investigated, when the maximum permissible tip-speed-ratio is limited in order to avoid the onset of cavitation.

2. Tidal turbine rotor designs

Two different tidal turbine rotors are investigated in this work. These rotors were derived from the original designs of Schluntz and Willden (2015) by Wimshurst and Willden (2016) and will be referred to as 'Rotor 1' and 'Rotor 2' respectively. Rotor 1 was designed to operate in a virtually unblocked domain (a blockage ratio of 0.0001), while Rotor 2 was designed to operate in a more highly blocked domain (a blockage ratio of 0.196). Here the 'blockage ratio' (B) refers to the ratio of the swept area of the rotor to the cross-sectional area of the computational domain that the device resides in. Both rotors were designed to achieve their maximum power coefficients at a tip-speed-ratio of 5 (the design tip-speed-ratio), in the domains they were originally designed for. In this work, the tip-speed-ratio λ is defined as $\lambda = \Omega R/U_\infty$, where Ω is the rotational speed of the rotor, R is the rotor radius and U_∞ is the freestream velocity (which is held constant at 2.0 m/s).

Fig. 1 shows the chord (c) and twist (β) distributions for Rotor 1 and Rotor 2. Both rotors use the same RISØ-A1-24 aerofoil along the entire span and have a total radius (R) of 10 m. The main difference between the rotor designs is that Rotor 2 has a greater local chord length and a slightly lower twist angle along the entire span. This allows it to apply greater thrust to the flow when operating at the same tip-speed-ratio as Rotor 1.

Inboard of $r/R = 0.25$, the RISØ-A1-24 aerofoil was blended into a cylinder to facilitate pitching at the blade root. A cylindrical nacelle with diameter $0.15D$ (where D is the rotor diameter), length $0.5D$ and a hemispherical nose cone, were also included in both rotor designs. These dimensions were chosen based on observations of some full-scale tidal turbine demonstrator devices that have already been installed (Belloni, 2013).

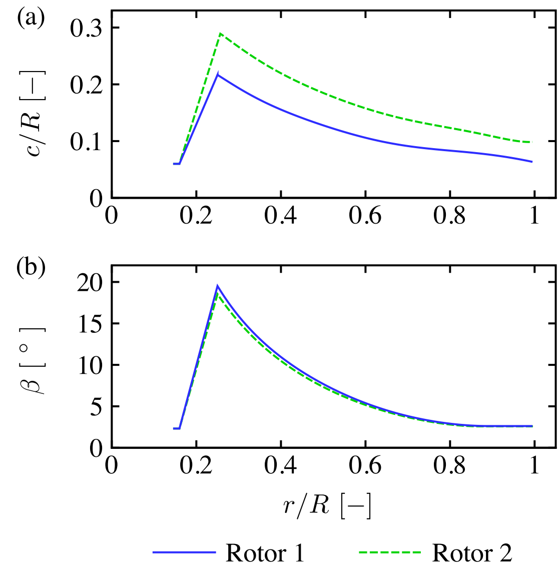

Fig. 1. Chord (a) and twist (b) distributions for Rotor 1 and Rotor 2. The rotor radius $R = 10$ m. The RISØ-A1-24 aerofoil is blended into a cylinder from $0.175 \le r/R \le 0.25$.

When analysed in a series of blade resolved computations by Wimshurst and Willden (2016), both rotors were found to achieve their maximum power coefficients close to the original design tip-speed-ratio of 5.0, in the domains they were originally designed for. More specifically, Rotor 1 achieved its maximum power coefficient in a low blockage domain (a blockage ratio of 0.01) at a tip-speed-ratio of 5.27, while Rotor 2 achieved its maximum power coefficient in a more highly blocked domain (a blockage ratio of 0.197) at a tip-speed-ratio of 5.18.

The blade resolved computations of Wimshurst and Willden (2016) will also be used for the cavitation analysis in this work. However, before presenting this analysis, some additional details of the blade resolved computations will be provided in the next section.

3. Blade resolved computations

The blade resolved computations were carried out in steady uniform flow, using the Multiple Reference Frame (MRF) approach of Luo et al. (1994) to simulate rotor rotation, over a range of blockage ratios (0.01, 0.065, 0.0982 and 0.197) and tip-speed-ratios (4–7). A freestream velocity (U_∞) of 2.0 m/s was adopted for all simulations and the rotational speed of the rotor was varied to set the tip-speed-ratio. To reduce the computational cost of each simulation, only a third of the rotor (a single blade and a section of the nacelle) was simulated in each computation. As shown in Fig. 2, the computational domain took the form of a 120° wedge shape, with periodic boundary conditions applied on the sides of the domain. The radius of the outer domain was varied to set the blockage ratio. The inlet turbulence intensity was set to 10.0%, with a turbulence length scale of 14 m, to mimic the high levels of turbulence found in real tidal channels, following Gant and Stallard (2008).

OpenFOAM (version 2.3.1) was used to solve the governing Reynolds-averaged Navier-Stokes (RANS) equations, with the $k-\omega$ SST turbulence model proposed by Menter (1994) for turbulence closure. Spatial convergence was assessed by refining the block structured mesh twice and then comparing the forces on a blade section at 95% of the blade span (between the three levels of refinement). With the coarsest mesh (2.1 million cells), the axial force per unit span (the thrust producing force) was within 0.37% of the finest mesh, while the tangential force per unit span was within 0.63% of the finest mesh (5.5 million cells). Hence, the coarsest mesh was deemed to be sufficiently accurate to compute the surface pressure distribution on the outboard blade sections. This mesh